Positional Accuracy of 3D Printed Quantum Emitter Fiber Couplers

Ksenia Weber, Simon Thiele, Mario Hentschel, Alois Herkommer, and Harald Giessen*

Precise positioning of optical elements plays a key role in the performance of optical systems. While additive manufacturing techniques such as 3D printing enable the creation of entire complex micro-objectives in one step, thus rendering lens alignment unnecessary, certain applications require precise positional alignment of the printing process with respect to the substrate. For example, in order to efficiently couple quantum emitters to single-mode fibers, which is a crucial step in the development of real world quantum networks, precise alignment between the emitter, the coupling optics, and the single-mode fiber is of utmost importance. In this work, the positioning accuracy of a Photonics Professional GT (Nanoscribe GmbH) 3D printing machine is evaluated by using the integrated piezo stage to align to gold markers that is manufactured via e-beam lithography. By running a statistical analysis of 38 printing cycles, a mean positional error of only 80nm is determined. Additionally, an entire system is 3D printed that can couple quantum emitters to optical single-mode fibers. Examining the focal spot of the 3D printed micro-optics, a positional accuracy of $\approx 1\,\mu m$ in all three dimensions is found, as well as excellent quality of the focal spot.

1. Introduction

The real world implementation of secure quantum communication is potentially one of the most impactful research topics in the field of quantum technology nowadays.[1–3] Making long-distance quantum communication networks a reality requires the implementation of a quantum repeater protocol.[4,5] This in turn

K. Weber, M. Hentschel, H. Giessen
4th Physics Institute and Research Center SCoPE
University of Stuttgart
Pfaffenwaldring 57, 70569 Stuttgart, Germany
E-mail: h.giessen@pi4.uni-stuttgart.de
S. Thiele, A. Herkommer
Institute of Applied Optics (ITO) and Research Center SCoPE
University of Stuttgart
70569, Pfaffenwaldring 9 Stuttgart, Germany
S. Thiele
Printoptix GmbH
70176, Johannesstr. 11 Stuttgart, Germany

necessitates a stable and reliable coupling mechanism of single-photon sources to optical single-mode fibers.[6–8] One way to realize such coupling is the use of a 3D printed micro-optical photon coupler produced via femtosecond 2-photon lithography.[9–12] This technique allows for a high degree of integration, offering a compact on-chip solution. However, so far high in-coupling efficiencies of the devices are lacking. One crucial condition to ensure high coupling efficiency to the single-mode fiber is the precise alignment of the 3D printed parts to the single-photon sources.[13,14] The possible deviations between the position of a quantum emitter and the focal spot of a micro-optical fiber coupling system in all three dimensions is illustrated in **Figure 1**.

In this work, we investigate the positioning accuracy of a Photonic Professional GT (Nanoscribe GmbH) 3D printing machine relative to pre-existing structures in order to evaluate its capabilities for the fabrication of single-mode fiber coupled single-photon sources. By using the machine's integrated piezo translation stage, we manually 3D-printed microstructures with respect to prefabricated gold (Au) markers. This process is similar to the one used during the fabrication of the single-mode on-chip fiber coupler presented in refs. [15, 16] In these works, a high-NA total-internal reflection (TIR) lens was printed directly onto a semiconductor quantum dot emitter. The TIR lens collected the intrinsically undirected light emission and transformed it into a mostly collimated beam, which was then focused onto the core of a single-mode fiber by another lens that is directly printed onto the end facet of the fiber. The fiber is held in place via a 3D-printed fiber holder and fixed with UV glue. The concept is illustrated in **Figure 2**. This two-lens approach has several advantages. First, the TIR lens enhances the single-photon extraction efficiency by decreasing the refractive index mismatch at the semiconductor sample surface and reduces the angle of the emitted single-photon light beam.[9,10,15] Second, the design is relatively robust against deviations of the fiber position.[13] We should mention that this solid fiber chuck concept gives better directional stability than for example clamp-based concepts.[14] As proven in,[16,17] our concept is also stable at cryogenic temperatures.

However, the design is highly sensitive to lateral misalignment between the TIR lens and the emitter. Indeed, in our previous works, we have achieved less than 25% coupling efficiency. For real-world quantum technology, one would rather like to achieve

**ADVANCED
SCIENCE NEWS**

www.advancedsciencenews.com

**ADVANCED
QUANTUM
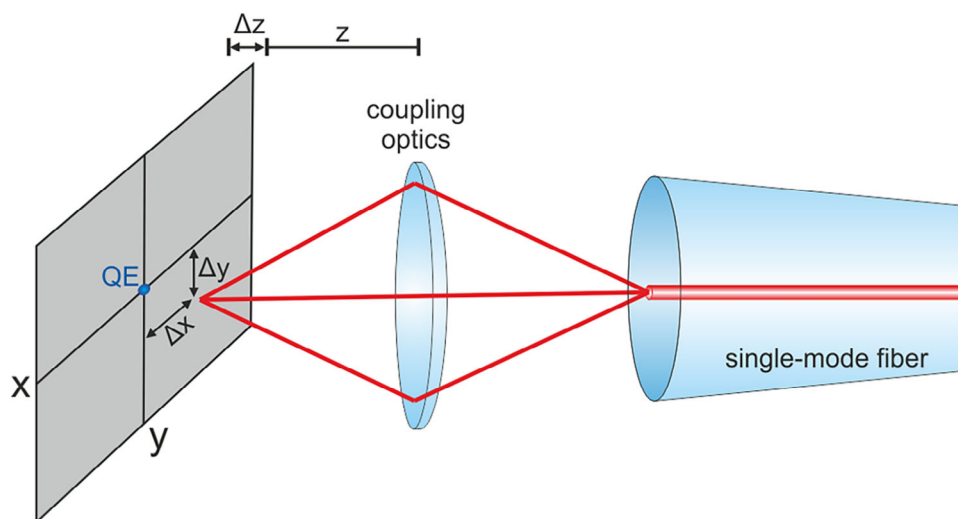TECHNOLOGIES**

www.advquantumtech.com

Figure 1. Schematic illustration of positional inaccuracy in fiber coupling of quantum emitters. Coupling optics are aligned to both the single-mode optical fiber and the quantum emitter (QE) on a substrate. Highlighted in the figure are the positional errors Δx, Δy, and Δz between the focal spot of the optics and the quantum emitter, resulting from inaccuracies during the fabrication process.
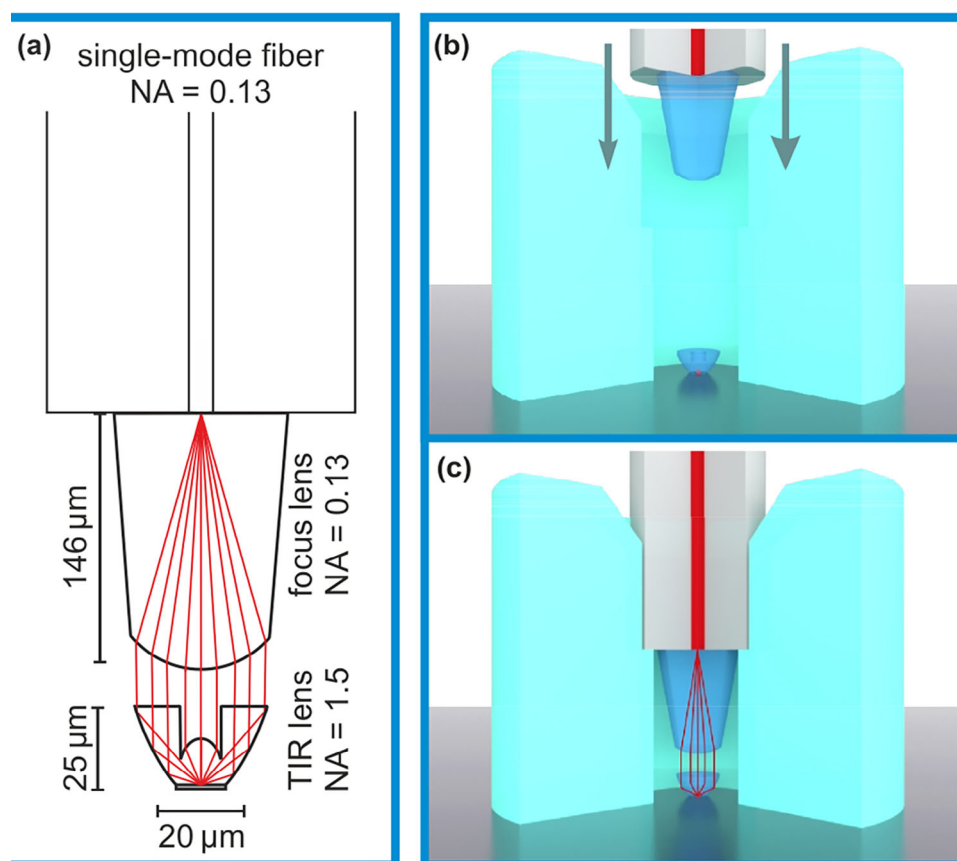

Figure 2. (a) Optical design to couple a single-mode fiber to a quantum emitter, obtained from sequential ray tracing. Light originating from the quantum emitter is collimated by a TIR lens (design NA = 1.5) and focused onto the core of the optical fiber by an NA matched (NA = 0.13) spherical focusing lens. Likewise, light that is emitted from the fiber is focused onto the quantum emitter. (b,c) Scheme displaying the integration of the optical fiber. Besides the two micro-lenses depicted in (a), a large cylindrical fiber chuck (shown in turquoise) is 3D printed onto the substrate. This chuck is precisely aligned to the TIR lens. The optical fiber is inserted into the chuck via a manual xyz-flexure stage (b), so that light from the quantum emitter is efficiently coupled into the fiber core via the micro-optical system and vice versa (c).
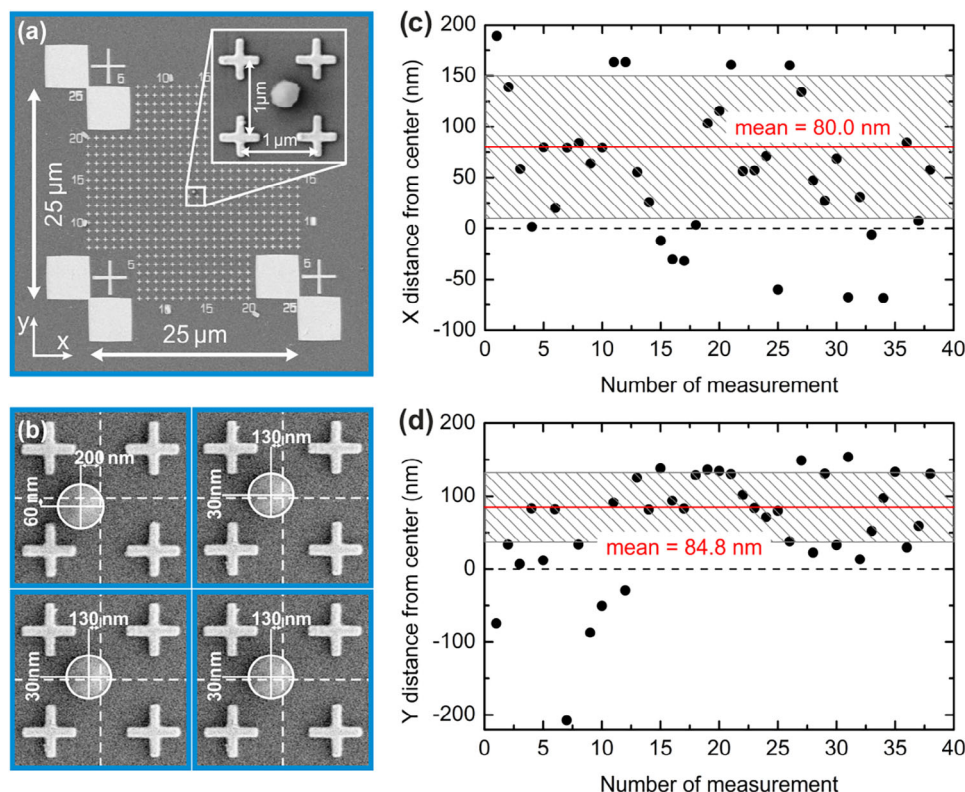
2400135 (2 of 6)

Figure 3. (a) SEM image of Au alignment markers after the 3D printing process. The inset indicates the position of the printed photoresist dot used to determine the positioning accuracy. (b) Exemplary SEM images of four different photoresist dots. (c,d) Statistical analysis of positioning accuracy of 38 3D printed dots, displaying their respective distance from the center of the alignment markers along the (b) x- and (c) y-direction. The dashed black line marks the zero line, while red line marks the (arithmetic) mean value. The shaded gray area highlights the standard deviation.

more than 90 or even 95% coupling efficiency to not lose too many single photons. Based on ray-tracing simulations, one can conclude that a positioning accuracy of <100 nm is required to avoid substantial loss of light intensity.[16] Since the entire single-mode fiber-coupler is produced in several printing steps, additional alignment errors can occur. This fact is schematically illustrated in Figure 1. We therefore not only quantify the positioning accuracy of a single printing step with the Photonic Professional GT, but also evaluate the alignment error of the entire lens system by measuring the 3D position of the system's focal spot.

2. Results and Discussion

First, we evaluate the positioning error of a single 3D printing step. To this end, we use a test marker structure as shown in **Figure** 3a. The markers are fabricated via standard electron beam lithography (Raith eLine Plus), evaporation of 3 nm Cr adhesion layer and a 50 nm gold film, and lift-off. During the alignment process, the writing laser of the 3D printing machine is switched on at a low power, and the integrated piezoelectric stage is used to overlap the focal spot of the laser with the diagonal intersection between the four pairs of Au squares. The target position is the center of these four points which is calculated from their measured piezo coordinates. By briefly switching on the laser at a higher intensity, a small photoresist dot is created at the calculated position. In order to determine the lateral (xy) offset

from the actual center of the square, we rely on scanning-electron microscopy (S-4800, Hitachi) in combination with the small Au crosses that were written between the alignment markers. These crosses are equally spaced at a distance of 1 µm apart from each other and thus define a grid that can be used to obtain the position of the 3D printed dot (see Figure 3a).

Out of 40 dots that were printed, only two lay outside of the central four crosses that mark the $1 \times 1 \, \mu m^2$ large center area of the square. Since in both of these cases, the error was uncharacteristically large (>2 µm) compared to the rest of the samples, it is assumed that those were most likely the result of human error, as all coordinates had to be entered manually. Since such errors do not reflect the actual accuracy of the process when it is performed correctly, we chose to neglect these two measurements. This leaves us with a total of 38 samples, all of which were positioned well within the central square of the test structure. Figure 3b,c shows the positioning error in x- and y-direction for the remaining 38 test prints. The mean positioning error was $\Delta x = 80$ nm with a standard deviation of $\sigma_x = 70$ nm in x- and $\Delta y = 84$ nm with a standard deviation of $\sigma_y = 48$ nm in y-direction. Please note that while Figure 3 shows both positive and negative values (corresponding to deviations in both directions), these numbers refer to the absolute value of the deviation, which is the relevant quantity here. The results indicate that in principal, a positional error well below 100 nm in one direction is possible and likely to achieve. However, due to
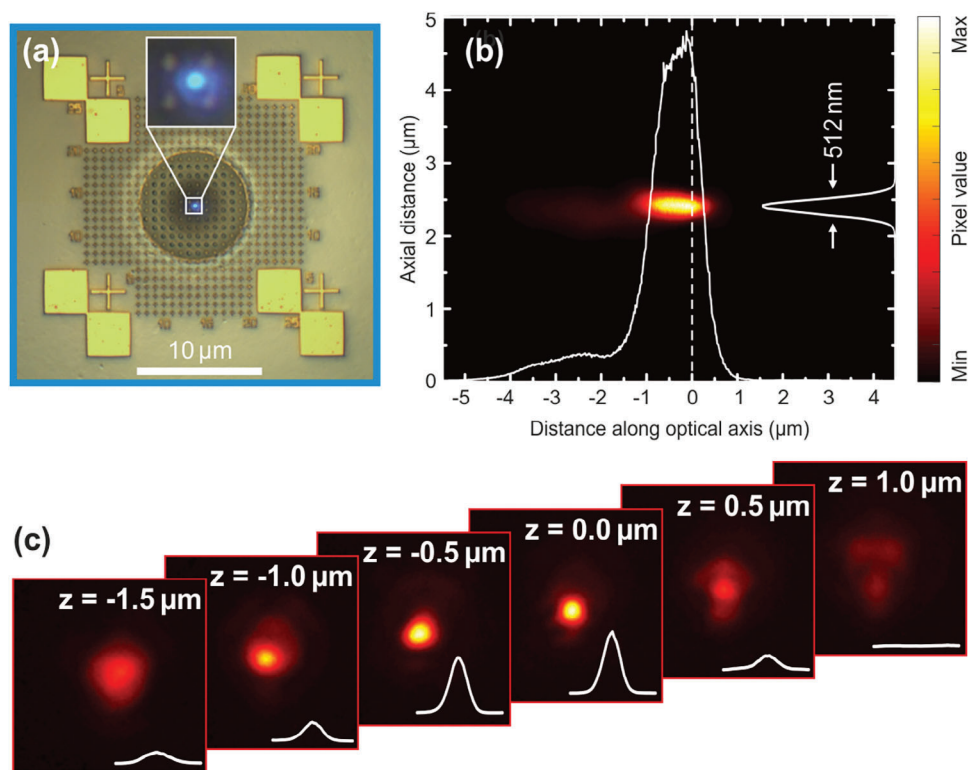
**ADVANCED
SCIENCE NEWS**

www.advancedsciencenews.com

**ADVANCED
QUANTUM
TECHNOLOGIES**

www.advquantumtech.com

Figure 4. (a) Microscope image which shows the Au markers after the fabrication of the 3D printed fiber coupler. The bright light spot in the center of the image is created when illuminating the back end of the single-mode fiber with white light. Inset shows the central $1 \times 1 \, \mu m^2$ square of the Au markers. (b) Beam profile measurement ($\lambda = 900$ nm) of fiber coupling optics. Dashed white line highlights the surface of the glass substrate. Solid white lines represent axial and lateral intensity cuts at the center of the beam and the focal plane respectively. Arrows mark the FWHM (512 nm). (c) Beam profiles at varying distances from the focal plane z. The surface of the substrate is located at $z = 0$. White lines in the bottom frames indicate the intensity distribution through the center of each spot.

the relatively large standard deviations, it cannot be guaranteed. Interestingly, while the positioning errors in x-direction appear to be more or less evenly distributed between positive and negative values, there seems to be a systematic error in the alignment along the y-direction. In this case, the vast majority of the dots (33 out of 38) are shifted in the positive direction ($\Delta y > 0$). This is also reflected in the substantially smaller standard deviation ($\sigma_y = 48$ nm vs $\sigma_x = 70$ nm). Investigating the cause of this error and compensating for it could be an important task in order to increase the alignment accuracy in the future. Possible error sources include misalignment of the laser in one direction, misalignment of one scanner axis, or visual error when determining the position of the laser spot relative to the alignment markers.

So far, only the positioning error of a single printing step, which corresponds for example to the positioning of the TIR lens on the quantum emitter in the actual device fabrication has been investigated. However, one also has to consider the positioning of the fiber lens onto the single-mode fiber, the positioning of the fiber chuck onto the TIR lens, and the positioning of the single-mode fiber inside the fiber holder when considering the entire device fabrication. In order to take all of these potential error sources into account, we fabricate an entire single-mode fiber-coupling device onto a transparent BK7 cover-slip with a test marker structure on top (see ref. [5] for details on the device fabrication). We then examine the quality of the device

by inverting the beam-path and investigating the output. To this end, we shine laser light at a wavelength of $\lambda = 900$ nm into the back end of the SM 780HP single-mode fiber. This corresponds to the path of the excitation laser during the single-photon fiber coupling experiments. We then observe the focal spot created by the micro-optical system through the transparent substrate via a 100× (NA 1.4) oil immersion objective. An additional imaging lens is inserted into the optical path of the microscope to increase the overall magnification to a factor of 150×. During the measurement, the glass substrate is fixed with scotch tape onto a sample holder which is mounted onto a 3D piezoelectric stage.

Figure 4a shows an exemplary microscope image during the measurement procedure. In the center of the Au marker structure, one can clearly observe a circle with a diameter of ≈10 μm which is the bottom of the TIR lens. In the center of this circle, the bright focal spot created by the lens system can be seen. Please note that 900 nm is in the NIR range and thus is outside of the operating wavelength of the utilized CCD camera. The spot is thus not depicted in real color and instead appears to be blue. On first inspection, the spot looks quite small with a well-defined centrosymmetric shape.

Furthermore, one can see that it is positioned well within the central $1 \times 1 \, \mu m^2$ square of the Au markers (the inset depicts a magnification of the central area of Figure 4a). We can thus

**ADVANCED
SCIENCE NEWS**
www.advancedsciencenews.com

**ADVANCED
QUANTUM
TECHNOLOGIES**
www.advquantumtech.com

conclude that the positioning accuracy of the entire fabrication process in the xy-plane is still below 1 μm.

Next, we investigate the shape and positioning accuracy of the focal spot in the z-direction (along the optical axis). In order to do so, we move the sample vertically in 20 nm steps, using the piezoelectric-stage. At each step, a camera image (without back light illumination) of the focal spot is recorded by the CCD camera. Images are saved in the uncompressed TIFF format. We then cut through the center of the focal spot and stitch the corresponding pixels together to obtain a through-focus image (shown in Figure 4b). The measured beam profile exhibits a near Gaussian shape with full width at half maximum (FWHM) of 512 μm. Also, peak intensity is reached close (≈ 100 nm) to the surface of the substrate (marked by the dashed white line), as intended by the design.

The precise alignment along the optical axis is illustrated in Figure 4c, where microscope images taken at different distances from the substrate's top surface as well as corresponding intensity patterns of the focal spot are shown. A clear defocusing of the laser spot accompanied by a distinct drop in peak intensity can be made out already at distances $\Delta z = 1$ μm away from the surface. This means that, just as intended, the focal plane of the fiber coupling optics overlaps with the top surface of the substrate. Since the light path is reversible, these results indicate that light emitted from a source close to the surface of the substrate is guided into the fiber core.

So far, the results of the through-focus measurements indicate high alignment accuracy of the entire 3D printed optical system. However, as we have seen before in the xy-positioning measurements, alignment errors can fluctuate to a significant degree from one manual alignment process to the next. Unfortunately, the fabrication of the full fiber-coupling system is too time-consuming to prepare a sufficiently large number of samples to perform a real statistical analysis of the z-displacement. One TIR lens printing takes ≈5 min, development takes 20 min, printing the chuck takes 45 min, development takes then 1 h, preparation (oxygen plasma), mounting, and printing of the fiber optics take another hour, preparation and fiber coupling and gluing and UV hardening takes 1–2 h, so that every single coupled fiber in a chuck takes ≈ 4–5 h. We instead choose to print seven identical TIR lenses onto a BK7 coverslip and illuminate them with a collimated laser beam ($\lambda = 900$ nm) at normal incidence. Since the focus lens on the fiber is designed to provide collimated illumination, this configuration should provide comparable results to the full coupling system.

Intensity distributions of the measured beam profiles are plotted in **Figure 5**. The mean position of the peak intensity was found to be located $\Delta z = -1.25$ μm above the substrate's surface with a standard deviation of $\sigma z = 0.29$ μm. All focal spots are found to be located fully within the TIR lens ($\Delta z > 0$), indicating that the actual focal length of the TIR lens is slightly shorter than the simulated one.

3. Conclusion

We investigated the positioning accuracy of the Photonics Professional GT (Nanoscribe GmbH) 3D printing machine for the fabrication of the single-mode fiber coupled single-photon source. Looking at 38 test samples, we found a lateral misalignment error
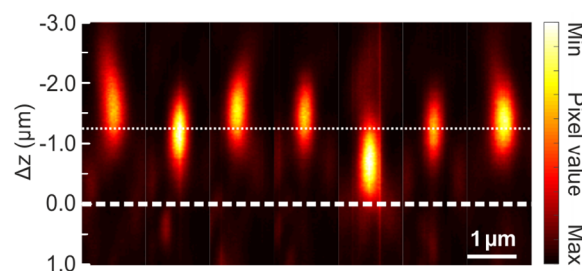

Figure 5. Through-focus intensity patterns of seven distinct TIR lenses illuminated with a collimated ($\lambda = 900$ nm) laser beam. The thick dashed line indicates the position of the substrate surface. The thin dotted line indicates the average Δz position of the highest intensity of the focal spots ($\Delta z = -1.25$ μm). Here, negative values of Δz correspond to a position in the TIR lens, while positive values correspond to a position in the substrate. Dimensions along the horizontal axis of each image are indicated by the scale bar.

of $\Delta x = 80$ nm with a standard deviation of $\sigma_x = 70$ nm in x- and a misalignment error of $\Delta y = 84$ nm with a standard deviation of $\sigma_y = 48$ nm in y-direction. When investigating the focal spot created by the full fiber coupling system, we found a well-defined spot profile with a FWHM of 512 μm and a lateral positioning accuracy below 1μm. Furthermore, when investigating the axial offset of the focal spots by illuminating seven distinct TIR lenses with a collimated laser beam, we found an average axial displacement of 1.25μm away from the target position with a standard deviation of $\sigma_z = 0.29$ μm.

In the future, we plan to use this knowledge to greatly enhance the efficiency of our single-mode on-chip fiber couplers. To reduce the lateral positioning error, one might start by compensating for the structural misalignment along the y-axis. Furthermore, we plan to automate the positioning process by implementing an alignment algorithm based on image recognition. Furthermore, the results of the TIR lens array measurements indicated that the focal length of the current design is ≈1 μm too short. We thus propose submerging the TIR lens into the substrate by that value to compensate the offset. Finally, thermo-optical effects that change the refractive index during cooling and structural shrinking while immersing the system into liquid helium should also be taken into account. These steps can help to greatly improve the efficiency of integrated single-mode fiber coupled single-photon sources and might thus play an important role in the realization of quantum communication networks of the future.

Our concept can also be applied to fiber coupling of light to single photon superconducting detectors.[18,19]

Acknowledgements

Conflict of Interest

The authors declare no conflict of interest.

Data Availability Statement

The data that support the findings of this study are available from the corresponding author upon reasonable request.

Keywords

3d printing, fiber coupling, micro-optics, quantum emitters

[1] F. Xu, X. Ma, Q. Zhang, H. K. Lo, J. W. Pan, *Rev. Mod. Phys.* **2020**, *92*, 25002.

[2] J. L. O'Brien, A. Furusawa, J. Vučković, *Nat. Photonics* **2009**, *3*, 687.

[3] J. Wang, F. Sciarrino, A. Laing, M. G. Thompson, *Nat. Photonics* **2020**, *14*, 273.

[4] P. van Loock, W. Alt, C. Becher, O. Benson, H. Boche, C. Deppe, J. Eschner, S. Höfling, D. Meschede, P. Michler, F. Schmidt, H. Weinfurter, *Adv. Quantum Technol.* **2020**, *3*, 1900141.

[5] F. Basso Basset, M. B. Rota, C. Schimpf, D. Tedeschi, K. D. Zeuner, S. F. Covre da Silva, M. Reindl, V. Zwiller, K. D. Jöns, A. Rastelli, R. Trotta, *Phys. Rev. Lett.* **2019**, *123*, 160501.

[6] F. Flamini, N. Spagnolo, F. Sciarrino, *Rep. Prog. Phys.* **2018**, *82*, 016001.

[7] P. Senellart, G. Solomon, A. White, *Nat. Nanotechnol.* **2017**, *12*, 1026.

[8] A. Boaron, G. Boso, D. Rusca, C. Vulliez, C. Autebert, M. Caloz, M. Perrenoud, G. Gras, F. Bussières, M. J. Li, D. Nolan, A. Martin, H. Zbinden, *Phys. Rev. Lett.* **2018**, *121*, 190502.

[9] P. I. Dietrich, M. Blaicher, I. Reuter, M. Billah, T. Hoose, A. Hofmann, C. Caer, R. Dangel, B. Offrein, U. Troppenz, M. Moehrle, W. Freude, C. Koos, *Nat. Photonics* **2018**, *12*, 241.

[10] A. Bogucki, Ł. Zinkiewicz, M. Grzeszczyk, W. Pacuski, K. Nogajewski, T. Kazimierczuk, A. Rodek, J. Suffczyński, K. Watanabe, T. Taniguchi, *Light Sci. Appl.* **2020**, *9*, 48.

[11] S. Fischbach, A. Schlehahn, A. Thoma, N. Srocka, T. Gissibl, S. Ristok, S. Thiele, A. Kaganskiy, A. Strittmatter, T. Heindel, S. Rodt, A. Herkommer, H. Giessen, S. Reitzenstein, *ACS Photonics* **2017**, *4*, 1327.

[12] J. K. Hohmann, M. Renner, E. H. Waller, G. von Freymann, *Adv. Opt. Mater.* **2015**, *3*, 1488.

[13] J. Schwab, K. Weber, L. Bremer, S. Reitzenstein, H. Giessen, *Opt. Express* **2022**, *30*, 32292.

[14] A. Bogucki, Ł. Zinkiewicz, W. Pacuski, P. Wasylczyk, P. Kossacki, *Opt. Express* **2018**, *26*, 11513.

[15] L. Bremer, C. Jimenez, S. Thiele, K. Weber, T. Huber, S. Rodt, A. Herkommer, S. Burger, S. Höfling, H. Giessen, S. Reitzenstein, *Opt. Express* **2022**, *30*, 15913.

[16] M. Sartison, K. Weber, S. Thiele, L. Bremer, S. Fischbach, T. Herzog, S. Kolatschek, M. Jetter, S. Reitzenstein, A. Herkommer, P. Michler, S. L. Portalupi, H. Giessen, *Light Adv. Manuf.* **2021**, *2*, 6.

[17] L. Bremer, K. Weber, S. Fischbach, S. Thiele, M. Schmidt, A. Kakganskiy, S. Rodt, A. Herkommer, M. Sartison, S. L. Portalupi, P. Michler, H. Giessen, S. Reitzenstein, *APL Photonics* **2020**, *5*, 106101.

[18] Y. Xu, A. Kuzmin, E. Knehr, M. Blaicher, K. Ilin, P.-I. Dietrich, W. Freude, M. Siegel, C. Koos, *Opt. Express* **2021**, *29*, 27708.

[19] S. Mennle, P. Karl, M. Ubl, P. Ruchka, K. Weber, M. Hentschel, P. Flad, H. Giessen, *Opt. Continuum* **2023**, *2*, 1901.